Battery Degradation in Control Algorithms for Redistribution of Benefits in a Community Energy Project

Inaesh Joshi
Supervisor(s): Valentin Robu, Peter Zhang, Sho Cremers
EEMCS, Delft University of Technology, The Netherlands

23-6-2022

Battery Degradation in Control Algorithms for Redistribution of Benefits in a Community Energy Project

Inaesh Joshi
Supervisor(s): Valentin Robu , Peter Zhang , Sho Cremers
EEMCS, Delft University of Technology, The Netherlands

Abstract

In a community energy project, batteries are the asset with the shortest lifespan and are therefore key contributors to cost. Understanding the influence of the battery state of health model on a control algorithm designed for redistribution of benefits in terms of financial gains in a community energy project can help elongate battery lifetime and reduce need for replacement hence minimising costs and reaping environmental benefits. Battery depreciation is predominantly stimulated by cyclic degradation and thus incurred costs are compared by simulating degradation curves for different battery storage systems in terms of chemistry and capacity. Costs are calculated by applying battery models to the control algorithm proposed by Norbu et al. (2021), which factors in cyclic degradation using the rainflow counting algorithm. The experiment explores the influences on cost of different battery chemistry types and capacities. Results demonstrate that lithium-ion batteries, which are the current norm in utility-scale applications, incur the lowest costs. Specifically, lithium manganese-oxide batteries appear to be most effective. Additionally, costs tend to decrease with increasing capacity until a minima corresponding to the optimal battery capacity.

1 Introduction

Concerns over climate change and the ongoing effort to diverge away from fossil fuels have birthed a deep interest in the deployment of a more sustainable and renewable energy system. A key research area within this topic has been community energy, otherwise coined citizen-driven renewable energy (Hewitt et al., 2019). This refers to the generation, storage and trade of energy within a community of prosumers (Norbu et al., 2021), each of whom may have partial ownership over the energy assets.

Over the past decade, academic interest in community energy has been gradually increasing (Creamer et al., 2018), which stems from the increase in deployment of community energy projects. An upward shift in global adoption of community energy projects is evident when sifting through the vast number of examples, ranging from community-owned wind turbines similar to those established on the Scottish Isles of Eigg or Gigha (Seyfang et al., 2012), to instituted projects in the Netherlands, Spain or Chile (Fuentes González et al., 2020). In the United Kingdom alone, over 300 successful community energy projects have been deployed, engaging over 90,000 local homes and businesses (Hydro, 2020). This general trend clearly highlights community energy as a key point of interest.

Community energy is incentivized by a plethora of both direct and indirect factors. From a humanitarian perspective, the employment of a renewable energy system yields clear environmental benefits; local communities are motivated to embrace this through favorable government policies, usually in the form of state support. For example, a range of government programs have been instigated to stimulate community-led energy initiatives in the United Kingdom (Seyfang et al., 2013). Another example is in Scotland where, as a part of its 2020 target, the government set a preliminary target of achieving 500 MW of community or locally-owned renewable electricity generation (Bomberg and McEwen, 2012). Community energy projects also facilitate decentralization of energy generation resulting in a more robust energy network, along with decreased financial costs if the energy generated is distributed optimally and fairly.

Obtaining maximal benefits in both financial and environmental dimensions requires a fair and optimal control algorithm, which is capable of allocating resources effectively. This paper focuses on the "heuristic-based battery control algorithm for maximization of behind-the-meter self-consumption" proposed by Norbu et al. (2021). This algorithm is rare in that it takes into consideration battery degradation, which is a critical component of a community energy system.

In a community energy project, energy may be generated and then stored in a battery storage system as a consumer may not demand power immediately upon generation. The schedule for energy supply and demand are not aligned.

Maintaining battery health can elongate battery lifespan, slowing down degradation and consequently the need for replacement, which reaps significant financial and environmental benefits. The rate of degradation can be affected by a multitude of factors including frequency of charge/discharge, depth of charge/discharge, battery storage unit technology,

and battery size. Battery degradation is a crucial consideration for efficient algorithm performance as the lifespan of this resource tends to be drastically shorter than other assets in an energy system. Thus, there is a need to establish a clear understanding of the model for battery state of health.

This paper explores how the model of the battery state of health influences the control algorithm designed for redistribution of benefits in a community energy project. To achieve this, the main focus is to analyze how different available batteries affect the decisions made by the control algorithm, after establishing an initial understanding of the battery state of health model proposed by Norbu et al. (2021). Based on these insights into battery degradation, the control algorithm may be built upon to attain fairer and more cost-efficient distribution of resources.

The structure of this paper is as follows: Section 2 provides an overview of the background behind batteries and the aforementioned control algorithm, followed by Section 3 which details the methodology utilised. Next, Section 4 outlines the results obtained. Section 5 considers the ethical aspects of this paper, and the results are then analysed and discussed in Section 6 together with any limitations and future improvements. Finally, a conclusion summarizing the findings in this paper is presented in Section 7.

2 Background

To develop an understanding of the model for battery state of health, it is first crucial to understand why batteries degrade and the factors that influence degradation rate, which are discussed in Section 2.1. Subsequently, Section 2.2 presents a range of battery energy storage technologies available in the market that must be considered as each option entails varying costs. As this paper is an extension of the work conducted by Norbu et al. (2021), Section 2.3 provides an overview of the control algorithm proposed - specifically closely related aspects such as the battery control algorithm and degradation model. Finally, other existing literature on battery degradation is acknowledged in Section 2.4.

2.1 Battery Degradation

Battery performance degrades over time, typically in the form of increased internal resistance or reduced maximum capacity. The rate of degradation tends to be affected by the environment as well as electrical usage (Chawla et al., 2010). For example, the thermal environment is a major factor in determining the finite lifetime of a battery as suboptimal temperatures can stimulate aging.

Evidence shows that useful battery lifetime is closely related to operational performance (Wang et al., 2016); the overall lifetime of a battery is significantly affected by its short-term operation. As such, the algorithm controlling battery operation is crucial for determining useful lifetime and thus cost.

Specifically, useful lifetime is dependent on the frequency of charge/discharge cycles and the depth of discharge, as stated by Yan et al. (2018). A single cycle refers to the process of discharging a battery down to any arbitrary state of charge (SoC) given any initial SoC, and then charging the battery up to some arbitrary SoC. The depth of discharge (DoD)

is the proportion of battery capacity that is discharged relative to the maximum capacity of the battery. For instance, the authors also state that "frequent and deep cycles accelerate cyclic aging and reduce the cycle life", which refers to the number of cycles that a battery can undergo based at a certain DoD before performance deteriorates. Alternatively, shallow and infrequent charge/discharge cycles correlate to a slower rate of cyclic aging, thus elongating battery calendar life.

Degradation curves, plotting typical cycle life versus DoD, can be obtained by repeatedly discharging a given battery to a specified DoD level, and then recharging it to its maximum capacity (Wang et al., 2016). Such type of cycles are referred to as regular cycles. However, in a community energy project with a battery energy storage system, cycles tend to be irregular. Irregular cycles refer to charge/discharge cycles where the battery is not recharged to full capacity; instead, it is recharged to an arbitrary SoC dictated by the control algorithm. Consequently, the battery state of health model must consider irregular cycles for an accurate depiction of cyclic aging. Degradation curves are acquired by the battery manufacturer through extensive experimentation in a controlled environment (at a specific temperature and C-rating). Therefore, it must be noted that such curves are not available for all battery types in the public domain.

2.2 Battery Energy Storage Technologies

Several types of battery energy storage technologies exist in the market today. A comprehensive study must consider the differences between these technologies in the context of a community energy project, as each entails different benefits and drawbacks.

Grid-scale battery energy storage systems (BESS) are the most widely utilised technology for wind farms (Wang et al., 2016). BESS offers "flexible charging-discharging characteristics", which allow for greater flexibility in a renewable energy system. However, they involve extremely high investment costs so a trade-off must be struck between battery performance and effort. Furthermore, sizing of energy systems in terms of capacity involve trade-offs between initial cost and cycle life cost, especially for BESS (Chawla et al., 2010). Due to their popularity in grid-scale projects, variations of BESS will be the focus of this paper.

In addition to capacity, battery storage systems can also be differentiated in terms of battery chemistry type, such as lithium-ion or lead-acid. Some key operational performance indicators of different chemistry types include battery lifespan, energy density, power/energy (P/E) ratio, and discharge times. It is important to note these values are not truly representative of battery performance, as performance is subject to the charge/discharge cycles as explained in Section 2.1. Asian Development Bank (2018) provides an overview of several battery chemistry types widely used in large-scale applications - a representative subset of which can be found in Table 1, with data on energy density and cycle life aggregated by Morris (2012) for comparison purposes. Financial cost estimations for battery chemistry types can be found in work conducted by Akinyele et al. (2017) and Mongrid et al. (2019).

While lead-acid batteries were previously the norm in large-scale applications, lithium-ion batteries have been dom-

Table 1: An overview of chemistry types for utility-scale batteries. (Asian Development Bank, 2018; Morris, 2012)

Comparison of Battery Chemistry Types		
Chemistry Type	Energy Density (Wh/kg)	Cycle Life
Lead-Acid (PbA)	35-50	250-1,000
Lithium-Ion (Li-Ion)	80-180	3,000
Nickel-Cadmium (Ni-Cd)	50-60	1,000-50,000
Nickel-Metal Hydride (Ni-MH)	60-80	300-600
Sodium-Sulfur (NaS)	150-240	2,500-40,000
Vanadium Redox Flow (VRB)	0-30	10,000

inating the market recently. This is emphasised by the fact that lithium-ion batteries accounted for almost 90% of large-scale battery storage additions in 2017 (IRENA, 2019). Lithium-ion batteries offer high energy and power densities, low discharge rates, and rapidly decreasing costs (Xu et al., 2018). It must be noted that several different subtypes exist for this chemistry. Examples of lithium-ion batteries include lithium manganese-oxide (LMO), lithium nickel-manganese-cobalt-oxide (NMC), lithium iron-phosphate (LFP), and lithium titanate (LTO).

2.3 Control Algorithm Proposed by Norbu et al., 2021

As mentioned in Section 1, Norbu et al. (2021) proposed a heuristic-based battery control algorithm in order to maximise the redistribution of benefits within a community energy project. This paper builds upon their work to gain insight into the model for battery state of health. As such, it is important to establish a basic understanding of the components of the algorithm that are associated with battery state of health: the battery control algorithm and the battery degradation model. Detailed descriptions of the summarised algorithms may be found in the aforementioned paper.

Battery Control Algorithm

The proposed battery control algorithm is a simple heuristic-based algorithm that charges the battery when there is an excess of power available, and discharges the battery when there is a deficit (i.e. prosumers demand more energy than is currently being generated). If the battery is at its maximum capacity the prosumer sells power to the central grid acquiring further financial benefits. Alternately, a cost is incurred if there is insufficient power being generated and the deficit in energy is not recoverable from the battery storage, in which case the prosumer must purchase energy from the utility grid.

Battery Degradation Model

As mentioned in section 2.1, it is important to consider both regular and irregular cycles when estimating battery degradation. As such, the model for battery state of health proposed employs a rainflow counting algorithm (Downing and Socie,

1982; Nieslony, 2022), which has been modified to determine regular and irregular cycles.

As an input, the rainflow counting algorithm takes the SoC profile obtained by simulating the battery control algorithm. Based on the output, which includes the number of cycles the battery has undergone thus far, a depreciation factor (DF) is calculated. The aforementioned cycles in the output are classified by type: differentiating between half or full cycles, and regular or irregular cycles. The overall DF is an aggregation of individual DFs for regular and irregular cycles. When the overall DF of the battery is equal to one, the battery requires replacement and hence a real-world financial cost is incurred.

The total cost in British Pounds (£) of a modelled community project is calculated by summing the operational cost and the cost incurred due to the battery, which is calculated via the following equation:

$$BatteryCost = \frac{V}{1000} * C * DF \qquad (1)$$

where:

V = battery capacity in kilowatt hours (kWh)
C = cost of battery per kWh in £

Currently, Norbu et al. (2021) only considers the lithium-ion battery in this degradation model. As such, this model is confined to a singular BESS technology, foregoing any potential insights alternatives may offer.

2.4 Other Related Literature

As operational performance is the largest determinant of battery degradation, most existing battery state of health models focus on cyclic degradation. Norbu et al. (2021) lists several such models of interest. For example, Yan et al. (2018) "incorporated dynamic battery life degradation in cost accounting model of energy storage system used for providing grid frequency regulation in the ancillary services market".

3 Methodology

This section presents and justifies the steps taken for the research, including any decisions made that may affect the outcome of the experiment. The approach explores how the model for battery state of health influences the control algorithm discussed in Section 2.3. Firstly, Section 3.1 explores how degradation curves have been applied to the control algorithm to replicate different battery models. Section 3.2 then discusses the regularisation of these curves, followed by Section 3.3 which mentions the datasets used in the experimental setup. Finally, Section 3.4 explains how different battery models have been compared to obtain insightful results.

3.1 Simulating Real-World Degradation Curves

Understanding how the battery state of health model affects a control algorithm for a community energy project requires experimentation with various model parameters. In particular, models may be differentiated with battery chemistry types. The chemistry influences the inherent characteristics of the battery and as such, contributes greatly to the cost of a community energy project as discussed in Section 2.2.

Degradation behaviour of battery chemistry types are represented in the form of degradation curves. By fitting data obtained from these curves into the existing control algorithm, the influence of battery chemistry on a community energy project may be observed in terms of cost. Unfortunately, available degradation data is often not easily processable as they are presented only as graphs in an image format. Precise data must be extracted for useful application in the control algorithm.

The battery state of health model detailed in Section 2.3 relies on a numerical representation of a lithium-ion degradation curve in order to calculate overall cost of a community energy project. This numerical representation involves a set of 100 individual values representing the expected number of cycles remaining in a battery's lifetime at a specified DoD. Each data point corresponds to a single DoD ranging from 1% to 100%; individually and manually extracting each of these data points for every degradation curve is not feasible.

Instead, a sample of representative data points (i.e. coordinates on the plots) was manually extracted from each degradation curve, reducing effort and the margin of human error. PlotDigitizer[1] was used to evaluate the coordinates of data points at regular intervals more accurately. By interpolating between the data points in this sample, a representative and applicable degradation curve was generated within the bounds of the control algorithm. In other words, the number of remaining cycles per DoD was simulated for every DoD from 1% to 100%, as required.
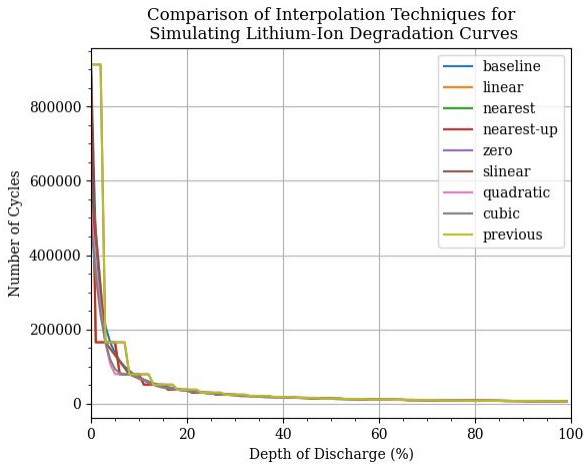

Figure 1: A comparison of interpolation techniques for simulating a li-ion degradation curve using a real-world curve.

Alternatively, degradation curves can be simulated by constructing mathematical formulas that resemble the real-world curves. However, this is a tedious process that requires extensive calibration. Additionally, curve trend-lines are not always representative of mathematical formulas which may lead to inaccuracies. The aforementioned interpolation technique allows for accurate trendlines as depicted in Figure 1, illustrating the degradation curves generated using interpo-

lation techniques in the *SciPy*[2] library by sampling 20 data points at equal intervals for the lithium-ion data used by Norbu et al. (2021). There is little difference in terms of curve behaviour when compared to the baseline curve, that precisely represents the original real-world degradation curve.

The most accurate interpolation technique was chosen by evaluating the error of the simulated curve when applying a given interpolation technique, compared to the baseline degradation curve used by Norbu et al. (2021). This error was measured in terms of RMSE (root mean-squared error) given by the following formula:

$$RMSE = \sqrt{\left(\frac{1}{n}\right) \sum_{n=1}^{n} (y_i - x_i)^2} \qquad (2)$$

where:

n = total number of DoD values (100)
y_i = cycles remaining when DoD = i for baseline curve
x_i = cycles remaining when DoD = i for simulated curve

As shown by Table 2, the 'cubic' interpolation technique was most accurate and was therefore chosen for the experiment. Although there is still an inevitable margin of human and simulation error, the main purpose of this paper is to objectively analyse how altering the battery state of health model influences the control algorithm. Relationships between different models are predominantly maintained through this technique, so the error can be considered negligible.

Table 2: A comparison of RMSE of interpolation techniques for simulating a li-ion degradation curve with a real-world curve.

RMSE of Interpolation Techniques	
Interpolation Technique	RMSE
Cubic	68680
Quadratic	70776
Linear	74371
Nearest	80730
Nearest-Up	80730
Zero	81057
Slinear	81057
Previous	81057

It is important to note that for the purpose of this experiment, a sample of 20 data points per degradation was arbitrarily chosen keeping in mind that a larger sample may stretch human effort, whereas a smaller sample may lead to further inaccuracies. Additionally, if the number of cycles was not present outside of certain bounds for the full required range of DoD from 0% to 100%, the data was extrapolated in order to maintain the general trend.

---

[1]https://plotdigitizer.com/

[2]https://scipy.org/

3.2 Regularisation of Degradation Curves

Data obtained on miscellaneous chemistry types is unfortunately inconsistent throughout sources as batteries are tested in various environments. For example, cycle life of batteries may vary drastically, especially if obtained at a different DoD. As such, degradation curves may be inaccurate relative to one another, which may inadvertently lead to inaccuracies in comparisons of the effects of battery models on the control algorithm.

Due to a lack of consistent information, a compromise must be made to obtain representative degradation curves and battery models for different battery chemistry types. To this end, regularisation was applied to the degradation curves in order to obtain comparable results. The following formula was utilised to regularise each data-point from the simulation degradation curve (i.e. each number of cycles remaining per DoD):

$$RegularisedCycles = N_i * \frac{3000}{N_1} * \frac{CL}{912748} \quad (3)$$

where:
N_i = number of cycles remaining at DoD i
N_1 = initial number of cycles at minimum (1%) DoD
CL = cycle life of battery chemistry

In this equation, 3,000 represents the cycle life of lithium-ion batteries according to table 1 and 912,748 is derived from the number of cycles remaining at 1% DoD for lithium-ion batteries according to the baseline. CL per battery chemistry is also derived from Table 1, with the most similar CL valuation utilised in order to ensure the fairest degradation comparisons possible by aiming for a similar initial number of cycles. This technique ensures that the relative differences in CL between battery chemistry types is maintained while retaining the trend of the respective degradation curves.

3.3 Simulation Datasets

Two datasets were chosen for community energy project simulations, both of which are collections of recorded energy demands during trials. The Thames Valley Vision (UKERC Energy Data Centre, 2020) dataset consists of 200 households over the timespan of one year, sampling consumption at intervals of thirty minutes. Alternatively, the Low Carbon London (UK Power Networks, 2013) dataset consists of 5,567 households over two and a half years, sampling at identical intervals. These energy demand profiles were input into the control algorithm to obtain cost estimations using a specified battery state of health model.

3.4 Comparing the Effect of Different Battery State of Health Models

As stated in Section 3.1, the research requires simulations with various model parameters to analyse the effect on the control algorithm and specifically cost. There are several battery-related parameters that can be manipulated, so that the model can accurately represent different BESS.

Different battery chemistry types exhibit varying degradation behaviour, hence why the experiment requires simulated degradation curves for specific chemistry types. Unfortunately, due to the extensive process manufacturers must undergo to obtain such curves, all real-world degradation data is not available in the public domain, which makes simulations all the more difficult. This presents a limitation to the research in the form of an inability to explore certain battery chemistry types within the context of a control algorithm, such as Vanadium Redox-Flow batteries. However, through extensive literature reviews, a representative set of degradation curves have been identified. These include lead-acid (Zhang et al., 2017), lithium-ion (Xu et al., 2018), nickel-cadmium (Boltta, n.d.), nickel-metal hydride (Adel et al., 2011) and sodium-sulfur (Rodrigues et al., 2014) batteries, for which costs were compared by applying the respective simulated degradation curves into the battery state of health model.

As Section 2.2 discussed, since lithium-ion batteries are the cutting-edge battery technology, it makes sense to inspect these in further detail. Specifically, lithium-ion chemistry subtypes were modelled in the existing infrastructure by simulating their respective degradation curves and comparing in terms of cost. Specifically, a comparison of the following lithium-ion batteries was carried out: lithium manganese-oxide, lithium nickel-manganese-cobalt oxide, and lithium iron-phosphate (Xu et al., 2018).

Additionally, to accurately model the battery chemistry types several other configurable parameters must be changed. Unfortunately, accurate values per battery chemistry for all parameters could not be found due to the dispersed nature of information on BESS. It was assumed that the initial battery capacity, power limit and minimum capacity remained constant throughout all battery state of health models and were thus considered the controlled variables within the experiment. Individual variables included battery cost per kilowatt hour (kWh), the expected lifetime of battery in years, cycle life and charging/discharging efficiency. The parameter values for simulations comparing battery chemistry were aggregated from various sources and can be found in Appendix A.

While the aforementioned simulations were run at a fixed battery capacity (5,000 times the number of prosumers in the respective dataset in terms of kWh), varying battery capacity for different BESS can offer additional insight as capacity is a significant contributor to cost and performance. Simulations were run for a representative set of battery chemistry types at specified capacities and then compared. The simulations were run for capacities ranging from 100kWH to 100000kWH. This wide range facilitates insights into the effect of battery sizing on the performance of a control algorithm.

4 Results

This section outlines the results obtained via the experiment previously described. Degradation curves simulations, which were subsequently applied to the battery state of health model, are illustrated in Section 4.1. In the subsequent sections, the performance of the control algorithm is compared in terms of cost for multiple battery models, which may differ in terms of chemistry or capacity, including several specific parameters.

4.1 Simulated Degradation Curves

As stated in Section 3.1, degradation curves were simulated in order to model different battery chemistry types. Regularisation was additionally applied in accordance with Section 3.2. Appendix B displays the degradation curves prior to regularization to illustrate the effect.

Figure 2 contains the simulated degradation curves for the five battery chemistry types upon which the experiment was run. As shown, Ni-MH clearly suffers from the lowest initial number of cycles at 1% DoD followed closely by PbA, while the remaining chemistries demonstrate similar initial values. The general trend for every chemistry is very similar, exhibiting decreasing trendlines with a greater negative gradient at a low DoD. Ni-Cd appears to degrade most gradually, albeit to a lower minimum number of cycles at a higher DoD. It should also be noted that all curves tend towards a similar number of cycles at a high DoD.

Appendix C contains a comparison of degradation curves for the selected lithium-ion subtypes. The figure illustrates that NMC degrades most rapidly followed by LFP, whereas LMO degrades at the slowest rate.
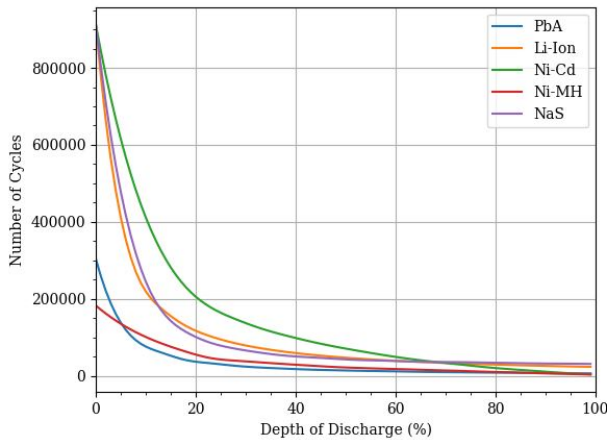

Figure 2: A comparison of battery degradation curves by chemistry.

4.2 Battery Chemistry

As detailed in Section 3.4, Table 3 presents the results of running the control algorithm at a fixed capacity for various battery chemistry types; battery chemistry types are presented in order of increasing costs for both datasets.

Li-ion batteries incur the lowest cost at £57,948.4 and £1,598,670 for the Thames and London datasets respectively, followed closely by NaS. There is a significant gap in term of cost between the aforementioned chemistries and PbA and Ni-Cd, as visually illustrated by the bar plots in appendix D. The most least effective chemistry appears to be Ni-MH, incurring a cost of £100,885 and £2,725,090 for the Thames and London datasets respectively.

Table 3: A comparison of community energy project costs by battery chemistry.

Comparison of Cost by Chemistry		
Chemistry Type	Cost for Thames Dataset (£)	Cost for London Dataset (£)
Li-Ion	57,948.4	1,598,670
NaS	65,790	1,810,280
PbA	72,048.4	1,968,870
Ni-Cd	79,434.2	2,154,800
Ni-MH	100,885	2,725,090

4.3 Lithium-Ion Battery Sub-Types

Similar to Section 4.2, Table 4 presents a comparisons of costs incurred by the control algorithm when utilising miscellaneous li-ion battery chemistry types within a community energy project.

All li-ion batteries appear to incur similar costs, indicated by the low range of costs resulting from usage of the various li-ion chemistries. The LMO battery seems to result in the lowest overall cost incurring £56,248.4 and £1,554,040 for the Thames and London datasets respectively, while the NMC battery appears to be the least effective chemistry type in terms of cost efficiency.

Table 4: A comparison of community energy project costs by li-ion battery chemistry.

Comparison of Cost by Li-Ion Battery Chemistry		
Li-Ion Sub-Type	Cost for Thames Dataset (£)	Cost for London Dataset(£)
LMO	56,248.4	1,554,040
LFP	57,298.4	1,581,610
NMC	66,904.5	1,743,320

4.4 Battery Capacities

Figures 3 and 4 illustrate the influence of battery capacity on the cost of a community energy project utilising a plethora of battery chemistries for capacities ranging from 100kWh to 100,000kWh, as detailed in Section 3.4.

Li-ion, NaS, and PbA batteries exhibit purely decreasing functions, although experimentation with higher battery capacities insinuate that the trendlines are, in fact, parabolic functions in that the control algorithm achieves a minimal cost at some optimal battery capacity. This parabolic nature is illustrated by the Ni-Cd battery for which cost decreases as capacity increases until 20,000kWh. Further evidence includes the gradually decreasing negative gradient of trendlines for li-ion, NaS, and PbA batteries, suggesting an approach to some minima. Upon comparing all aforementioned chemistries, li-ion batteries seem to be the most cost-efficient chemistry at any given capacity, while Ni-Cd appears to be the least.

An anomaly occurs for Ni-MH batteries as it exhibits a strictly increasing function in terms of cost incurred as battery
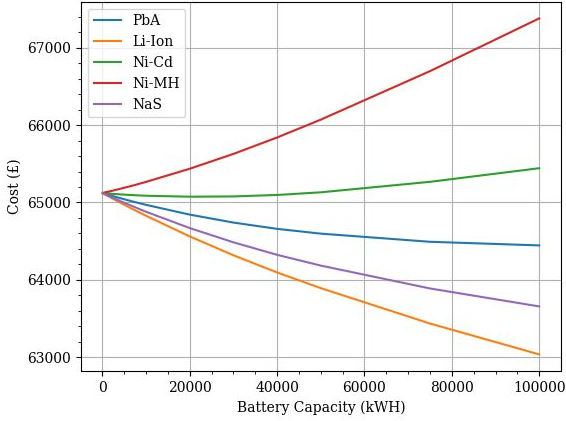
Figure 3: Cost vs. battery capacity and chemistry for the Thames Valley Vision dataset.
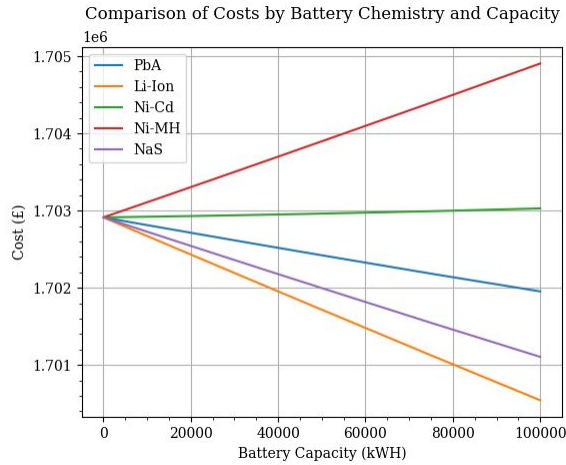

Figure 4: Cost vs. battery capacity and chemistry for the Low Carbon London dataset.

capacity simultaneously increases. Additionally, the magnitude of the positive gradient of the trendline for Ni-MH batteries continuously increases with higher battery capacities implying that the chemistry is extremely cost-inefficient.

It must be noted that at first glance the results from the London dataset in Figure 4 appears to demonstrate a more linear trendline comparing cost and capacity for all battery chemistry types, in the sense that the magnitude of the gradients are comparatively lower. However, this can be attributed to the amplified cost incurred in this dataset due to a higher number of prosumers participating in the community energy project; a closer inspection with magnified trendlines will reveal similar trendlines to Figure 3.

5 Responsible Research

Responsible research involves the consideration of several ethical facets. Firstly, to ensure reproducibility of results the paper describing the control algorithm which the exper-

iments were performed on has been referenced to allow third parties to replicate the results personally. Additionally, the datasets used have been mentioned in Section 3.3 and the battery model parameters for the experiment have been explicitly included in Appendix A. To actually conduct the experiment, the setup can be easily reproduced using the methodology described in Section 3.

Regardless of presumptions, all results have been included to guarantee data inclusivity and transparency. These results are predominantly presented in Section 4, although complementary data has been included in the appendix.

From an ethical perspective, it is crucial to acknowledge the limitations of the research, which are detailed in Section 6.2. Cost valuations of community energy projects derived from the application of various battery models on the control algorithm are purely experimental; these valuations should not be considered accurate to any specific real-world community energy initiative as each project is situationally specific and costs can different due to several different factors. This paper purely analyses the effect of different battery models on a control algorithm redistributing benefits within a community energy project, in order to gain insights into the battery state of health model that may be leveraged for maximisation of financial and environmental benefits gained.

6 Discussion

The following section discusses the results obtained in relation to the research question, taking into account background knowledge and comparability to existing literature. Section 6.2 then considers notable limitations of the experiment and explores any possible future improvements or extensions to the research.

6.1 Analysis of Results

Various battery models have been applied to the control algorithm in order to observe the effect in terms of performance, which is measured by cost. Battery chemistry types differ significantly through multiple facets - the most pivotal of which is cyclic degradation. An analysis of the simulated degradation curves in Figure 2 indicates that some battery chemistry types have more favourable degradation characteristics, which is expected to be reflected in terms of cost incurred by the control algorithm in a community energy project.

The Ni-MH battery chemistry suffers from the lowest number of cycles at a low DoD of 1% with just under 200,000 cycles expected. While the chemistry degrades at a slower rate than alternatives, it consistently exhibits the lowest number of cycles at any given DoD below a relatively high DoD. In combination with a comparatively low average lifetime of 5 years, this suggests higher costs will be incurred - a hypothesis that is supported by the high cost valuations of £100,885 and £2,725,090 for the Thames and London datasets respectively in Table 3 for a community energy project utilising Ni-MH batteries. These costs indicate that the Ni-MH battery is an estimated 27.9% less effective than the alternative closest in terms of performance (Ni-Cd) and 70.3% less effective than the best alternative (li-ion). The aforementioned proportional comparisons were obtained by averaging the fractional

differences in terms of cost for the two datasets between the relevant battery chemistry types. Ultimately, the results imply that investing in a Ni-MH BESS may not produce any financial benefits, as Figures 3 and 4 suggest that costs continuously increases with battery capacity. This seems counterintuitive for BESS available in the market as a complete absence of benefits renders the technology futile, so the results could possibly be attributed to the limitations discussed in Section 6.2. However, it can be noted that the Ni-MH chemistry is the least effective battery model when compared to the batteries experimented with.

The degradation behaviour of Ni-Cd batteries is unique in the sense that it boasts a relatively slow degradation rate at lower DoD, while demonstrating some of the lowest number of cycles at DoD higher than 85%. While enjoying a high initial number of cycles of around 800,000 at 1% DoD, results indicate that Ni-MH batteries are only more cost-efficient than Ni-Cd batteries. This is especially surprising when considering that cyclic degradation is considered a highly influential factor of cost. PbA batteries demonstrate the second lowest number of cycles at 1% DoD at around 300,000 cycles, with rapid degradation at a low DoD before plateauing at a higher DoD. This would initially imply that Ni-Cd batteries are superior to PbA batteries in terms of cost incurred due to lower cyclic degradation, which is not the case. In fact, costs of a community energy project utilising PbA batteries tend to decrease more rapidly with cost, while projects using Ni-Cd batteries gravitate to a higher minimal cost at a lower capacity. This is likely a result of the significantly higher cost per kWh of Ni-Cd batteries at £400 per kWh compared to £216 per kWh for PbA batteries, indicating market cost of batteries is a significant factor of the battery model that influences the control algorithm.

On the positive end of the spectrum, li-ion batteries appear to be most effective in terms of cost, closely followed by NaS batteries. Both chemistry types demonstrate extremely similar regularised degradation curves and high average lifetimes of 20 and 15 years for li-ion and NaS batteries respectively. Some additional differences lie in the battery costs per kWh and charging/discharging efficiency, with lithium-ion batteries costing £150 per kWH at 0.85% efficiency and NaS batteries costing £250 per kWH at 0.89% efficiency. These superior characteristics of both battery models and the high initial cycle life of above 800,000 cycles at 1% DoD point to a profitable influence on the control algorithm. In fact, li-ion batteries are an estimated 11.8% more cost efficient than the next best alternative of NaS. In turn, NaS batteries are an estimated 8.4% more effective than its next best alternative, which is PbA. Figures 3 and 4 illustrate that community energy projects operating with li-ion, NaS and PbA batteries all decrease in terms of cost as capacity increases, although at a decreasing rate as it approaches higher capacities. This indicates some minimum cost will be acquired at some optimal capacity; this theory is further supported by Equation 1, since it intuitively implies that the cost incurred due to the battery increases with capacity. It would be unreasonable to surmise that costs simply continue to decrease infinitely as this would indicate that costs becomes negligible at some high battery capacity, which an economic impossibility. The

satisfactory performance of PbA batteries supports the fact that PbA batteries were previously the chemistry of choice for many utility-scale applications. Furthermore, the superiority of li-ion batteries is inline with the recent dominance of li-ion BESS in the market, as evidenced in Section 2.2.

A comparison of lithium-ion subtypes reveals that the LMO battery is most cost-effective, closely followed by LFP differing in terms of cost by only an estimated 1.8%. NMC batteries appear to incur the highest costs, differing from LFP batteries by an estimated 11.8%. The positive effect of the LMO battery may be attributed to the low cost per kWh at £116 and slower degradation rate, demonstrating a comparatively higher number of cycles as DoD increases. Although the cyclic degradation behaviour of the NMC battery is actually more favourable, it incurs a higher cost than LFP; this can be explained by the higher cost per kWh at £160 compared to £137 for LFP batteries. It must also be noted that the cost incurred for all li-ion subtypes does not diverge notably from the results of the li-ion model used in Section 4.2, thus reinforcing the validity of the experiment.

6.2 Limitations and Future Work

A key limitation of this research includes the plethora of BESS available in the market. It would be unfeasible to model all BESS available and, as such, a representative subset of battery models were chosen. A lack of literature and data on certain battery characteristics also meant that assumptions had to be made on certain variables. A possible extension of this paper would be an analysis of the influence of further battery models, perhaps by way of additional battery chemistry types. To this end, simulations may be conducted for BESS which lack information in the public domain. An example of an untested technology includes vanadium redox-flow batteries for which a publicly available degradation curve was not located.

Additionally, data on different BESS drastically differ between sources due to different testing environments and variations in manufacturers. For example, degradation behaviour or cycle life of any given battery chemistry may vary if tested at inconsistent temperatures or a non-identical DoD. As such, experimental parameters entail a degree of uncertainty and data used to model batteries may be inaccurate relative to other used information. To this end, regularisation techniques were used to normalise the dataset and diminish the negative effects of data inconsistencies. However, it is extremely difficult to completely remove relative differences in data and thus it is crucial to acknowledge this limitation. A suggestion for future work includes experimentation with different regularisation techniques to obtain accurate battery models.

The insights derived in this paper are intended to be leveraged for improvements in a control algorithm for community energy projects. A possible extension of this work could be the adaptation of the algorithm based on various battery models with the aim to minimise costs incurred due to battery degradation. As a suggestion, machine learning models may be applied to predict degradation based on a variety of configurable inputs, ranging from degradation behaviour to market costs of a battery. This learning model, alongside prosumer consumption profiles, may then be exploited to alter the bat-

tery control algorithm to maximise battery lifetime and minimise need for replacement.

7 Conclusion

This paper explores how the model of the battery state of health influences the control algorithm designed for redistribution of benefits in a community energy project. This is achieved by applying various battery models to the control algorithm designed by Norbu et al. (2021) and comparing costs incurred. In particular, the paper differentiates between models in terms of battery chemistry and capacity, which indirectly includes several other configurable parameters such as battery lifetime or efficiency. A key discriminator between battery chemistry types includes degradation behaviour, which may be modelled in the form of degradation curves. As cyclic degradation is a highly influential factor determining battery lifetime and thus cost, these curves were simulated and input into the different models. Costs incurred by the battery are calculated by determining a depreciation factor, derived using a rainflow counting algorithm. Results indicate that li-ion batteries are the most cost-effective, followed by NaS, PbA, Ni-Cd, and Ni-MH batteries in order of decreasing costs. Focusing on li-ion battery sub-types, it appears that the LMO chemistry incurs the lowest cost, followed by LFP and NMC respectively. Costs also tend to decrease as battery capacity increases, although at a decreasing rate implying a minimal cost will be achieved for differing BESS at some optimal capacity. Ni-MH batteries are an anomaly, in that investments into this chemistry appear to be futile due to increasing costs coinciding with increasing capacity. Major determinants of these cost valuations are cyclic degradation, battery cost per kWh, and expected lifetime. It must be noted that data on battery models are lacing and inconsistent due to varying testing environments, which lead to several assumptions for the experiment. The insights obtained provide relative comparisons between battery models and the influence on the control algorithm, which may be leveraged to improve the algorithm by elongating battery lifetime and thus minimising costs.

References

Adel, B., Youtong, Z., & Shuai, S. (2011). Simulation and comparison of hev battery control for best fuel economy and longer battery life. *World Electric Vehicle Journal*, *4*, 421–426. https://doi.org/10.3390/wevj4020421

Akinyele, D., Belikov, J., & Levron, Y. (2017). Battery storage technologies for electrical applications: Impact in stand-alone photovoltaic systems. *Energies*, *10*. https://doi.org/10.3390/en10111760

Asian Development Bank. (2018). Handbook on battery energy storage system. *Asian Development Bank*. https://doi.org/http://dx.doi.org/10.22617/TCS189791-2

Beltran, H., Ayuso, P., & Pérez, E. (2020). Lifetime expectancy of li-ion batteries used for residential solar storage. *Energies*, *13*, 568. https://doi.org/10.3390/en13030568

Boltta. (n.d.). Nickel-cadmium. *Boltta*. http://boltta.com/nickel-cadmium/

Bomberg, E., & McEwen, N. (2012). Mobilizing community energy. *Energy Policy*, *51*, 435–444. https://doi.org/https://doi.org/10.1016/j.enpol.2012.08.045

Breeze, P. Chapter 10 - power system energy storage technologies (Third Edition). In: *Power generation technologies (third edition)* (Third Edition). Third Edition. 2019, pp. 219–249. ISBN: 978-0-08-102631-1. https://doi.org/https://doi.org/10.1016/B978-0-08-102631-1.00010-9.

Chawla, M., Naik, R., Burra, R., & Wiegman, H. Utility energy storage life degradation estimation method. In: *2010 ieee conference on innovative technologies for an efficient and reliable electricity supply*. 2010, 302–308. https://doi.org/10.1109/CITRES.2010.5619790.

Climatebiz. (2022). Lifepo4 battery (expert guide on lithium iron phosphate).

Creamer, E., Eadson, W., van Veelen, B., Pinker, A., Tingey, M., Braunholtz-Speight, T., Markantoni, M., Foden, M., & Lacey-Barnacle, M. (2018). Community energy: Entanglements of community, state, and private sector. *Geography Compass*, *12*. https://doi.org/https://doi.org/10.1111/gec3.12378

Downing, S. D., & Socie, D. F. (1982). Simple rainflow counting algorithms. *International journal of fatigue*, *4*(1), 31–40.

Fuentes González, F., van der Weijde, A. H., & Sauma, E. (2020). The promotion of community energy projects in chile and scotland: An economic approach using biform games. *Energy Economics*, *86*, 104677. https://doi.org/https://doi.org/10.1016/j.eneco.2020.104677

Hewitt, R. J., Bradley, N., Compagnucci, A. B., Barlagne, C., Ceglarz, A., Cremades, R., McKeen, M., Otto, I. M., & See, B. (2019). Social innovation in community energy in europe: A review of the evidence. https://doi.org/https://doi.org/10.3389/fenrg.2019.00031

Hydro, S. (2020). Community energy: State of the sector 2020. *Community Energy England, Community Energy Wales, Scene*.

IRENA. (2019). Innovation landscape brief: Utility-scale batteries. *International Renewable Energy Agency*.

Large. (2021). Battery cost per kwh - materials and comparison.

Mongird, K., Viswanathan, V., Balducci, P., Alam, J., Fotedar, V., Koritarov, V., & Hadjerioua, B. (2019). Energy storage technology and cost characterization report. *HydroWIRES*.

Morris, M. (2012). Comparison of rechargeable battery technologies. *ASME Early Career Technical Journal*, *11*, 148–155.

Nieslony, A. (2022). Rainflow counting algorithm. *MATLAB Central File Exchange*. https://www.mathworks.com/matlabcentral/fileexchange/3026-rainflow-counting-algorithm

Norbu, S., Couraud, B., Robu, V., Andoni, M., & Flynn, D. (2021). Modelling the redistribution of benefits from

joint investments in community energy projects. *Applied Energy*, *287*. https://doi.org/10.1016/j.apenergy.2021.116575

Rodrigues, E., Fernandes, C., Godina, R., Abebe Worke, B., & Catalão, J. Nas battery storage system modeling and sizing for extending wind farms performance in crete. In: 2014. https://doi.org/10.1109/AUPEC.2014.6966547.

Seyfang, G., Park, J. J., & Smith, A. (2013). A thousand flowers blooming? an examination of community energy in the uk. *Energy Policy*, *61*, 977–989. https://doi.org/https://doi.org/10.1016/j.enpol.2013.06.030

Seyfang, G., Park, J. J., & Smith, A. (2012). Community energy in the uk.

Susarla, N., & Ahmed, S. (2020). Estimating the cost and energy demand of producing lithium manganese oxide for li-ion batteries. https://doi.org/https://doi.org/10.2172/1607686

UK Power Networks. (2013). Smartmeter energy consumption data in london households. *UK Power Networks*. https://data.london.gov.uk/dataset/smartmeter-energy-use-data-in-london-households

UKERC Energy Data Centre. (2020). Thames valley vision end point monitor data. *UKERC*. http://www.thamesvalleyvision.co.uk/

Wang, F., Deng, Y., & Yuan, C. (2020). Design and cost modeling of high capacity lithium ion batteries for electric vehicles through a techno-economic analysis approach. *Procedia Manufacturing*, *49*. https://doi.org/10.1016/j.promfg.2020.06.006

Wang, Y., Zhou, Z., Botterud, A., Zhang, K., & Ding, Q. (2016). Stochastic coordinated operation of wind and battery energy storage system considering battery degradation. *Journal of Modern Power Systems and Clean Energy*, *4*, 104677. https://doi.org/https://doi-org.tudelft.idm.oclc.org/10.1007/s40565-016-0238-z

Xu, B., Oudalov, A., Ulbig, A., Andersson, G., & Kirschen, D. S. (2018). Modeling of lithium-ion battery degradation for cell life assessment. *IEEE Transactions on Smart Grid*, *9*(2), 1131–1140. https://doi.org/10.1109/TSG.2016.2578950

Yan, G., Liu, D., Li, J., & Mu, G. (2018). A cost accounting method of the li-ion battery energy storage system for frequency regulation considering the effect of life degradation. *Protection and Control of Modern Power Systems*, *3*. https://doi.org/10.1186/s41601-018-0076-2

Zhang, P., Liang, J., & Zhang, F. (2017). An overview of different approaches for battery lifetime prediction. *IOP Conference Series: Materials Science and Engineering*, *199*, 012134. https://doi.org/10.1088/1757-899X/199/1/012134

Zhu, W. H., Zhu, Y., Davis, Z., & Tatarchuk, B. J. (2013). Energy efficiency and capacity retention of ni–mh batteries for storage applications. *Applied Energy*, *106*, 307–313. https://doi.org/https://doi.org/10.1016/j.apenergy.2012.12.025

A   Battery State of Health Model Parameters

Table 5: An overview of the parameters used for different battery chemistry types in the battery state of health model to obtain estimations of costs incurred in a community energy project.

Parameters for Battery Chemistry Types			
	Battery Chemistry		
Parameter	PbA	Li-Ion	Ni-Cd	Ni-MH
Cost (£/kWh)	216	150	400	250
Lifetime (Years)	10	20	15	5
Cycle Life	1000	3000	3000	600
Charging Efficiency (%)	0.85	0.85	0.7	0.82
Discharging Efficiency (%)	0.86	0.85	0.7	0.82
Minimum Capacity (kWh)	0.2	0.2	0.2	0.2
Initial Battery Capacity (kWh)	0.6	0.6	0.6	0.6
Power Limit (%)	0.5	0.5	0.5	0.5
	Battery Chemistry		
Parameter	NaS	LMO	NMC	LFP
Cost (£/kwH)	250	116	160	137
Lifetime (Years)	15	10	16	21
Cycle Life	3000	3000	3000	3000
Charging Efficiency (%)	0.89	0.85	0.85	0.85
Discharging Efficiency (%)	0.89	0.85	0.85	0.85
Minimum Capacity (kWh)	0.2	0.2	0.2	0.2
Initial Battery Capacity (kWh)	0.6	0.6	0.6	0.6
Power Limit (%)	0.5	0.5	0.5	0.5

It must be noted that the parameters derived to be used in the experiment depicted in table 5 were collected from a variety of sources (Asian Development Bank, 2018; Large, 2021; Morris, 2012; Zhu et al., 2013; Breeze, 2019; Susarla and Ahmed, 2020; Beltran et al., 2020; Wang et al., 2020; Climatebiz, 2022).

B   Degradation Curves Before Regularization

Figure 5 displays the degradation curves for battery chemistry types prior to regularization. This highlights the effect of regularization when comparing the curves to figure 2.
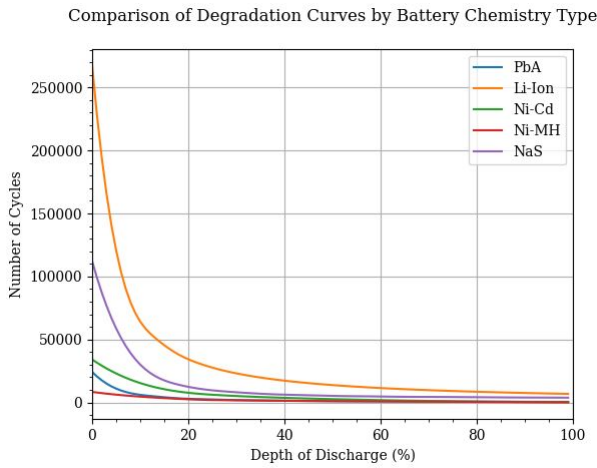
Figure 5: A comparison of battery degradation curves by chemistry prior to regularization, demonstrating the drastic differences in initial number of cycles at a minimal DoD of 1% between curves.
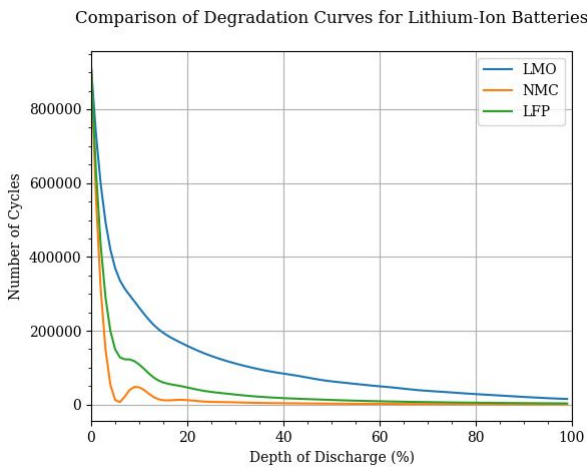
C   Lithium-Ion Degradation Curves

Figure 6: A comparison of battery degradation curves for a representative subset of lithium-ion chemistry types.

D   Comparison of Costs by Chemistry Type

Figures 7 and 8 intend to visually demonstrate the difference in costs incurred when applying battery models using different chemistry types to the control algorithm for redistribution of benefits within a community energy project. In particular, the similarly low costs of li-ion and NaS is noticeable, closely followed by PbA and Ni-Cd. Meanwhile, Ni-MH incurs drastically higher costs.
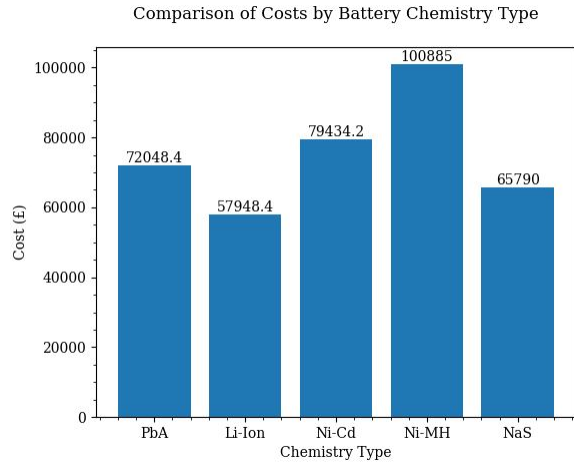
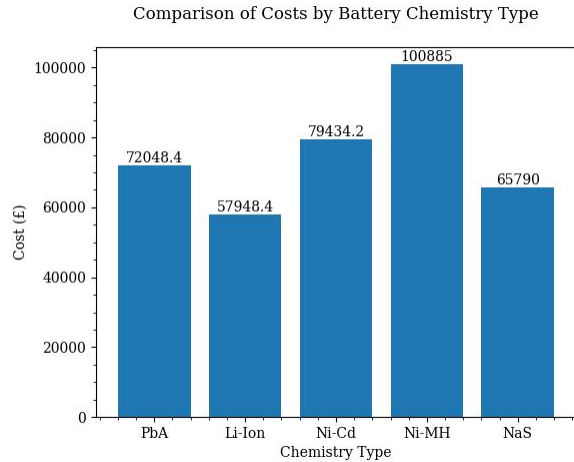Figure 7: Estimated costs per battery chemistry for Thames Valley Vision dataset.

Figure 8: Estimated costs per battery chemistry for Low Carbon London dataset.